# INITIAL STAGE OF CUBIC BORON NITRIDE GROWTH BY LOW PRESSURE ICP–CVD

Takanori Ichiki, Satoshi Amagi and Toyonobu Yoshida

*Department of Metallurgy and Materials Science*
*Faculty of Engineering, The University of Tokyo*
*7-3-1 Hongo, Bunkyo-ku, Tokyo 113 , Japan*

## Abstract

In order to investigate the growth mechanism of cubic boron nitride (*c*-BN) from the vapor phase, investigations have been carried out concerning the evolution of the crystalline structure, the surface composition and the morphology of deposited films at different growth stages. BN films with thickness gradients in lateral direction were deposited on Si substrates by using low pressure ICP–CVD. Characterizations of the film surface were carried out at various lateral positions on the substrate by using FT-IR, XPS, AES, RHEED and AFM. Results have been mainly discussed with regard to the initial stage of the *c*-BN growth.

## 1 Introduction

We have developed a novel chemical vapor deposition process using low pressure ICP and have deposited cubic boron nitride (*c*-BN) films successfully by this process [1–4]. It is known that ion bombardment during deposition is essential for the *c*-BN growth, but its role in the *c*-BN formation is still unknown. Clarifying the growth mechanism of *c*-BN is of great importance not only as a subject of basic science but also as a guide for the improvement of the film quality.

For better understanding of the growth mechanism, we have attempted to obtain microscopic informations of *c*-BN films at different growth stages. For this purpose, it is desirable to prepare films with different thickness under similar deposition conditions. In the case of laser deposition, for example, a half-shadow technique has been reported to permit the preparation of films with lateral thickness gradients [5]. However, this technique can not be applied to the ion-assisted deposition techniques since a shutter has different influence on ions and neutrals. By applying a *plasma diffusion technique* to prepare films by plasma CVD, thin *c*-BN films with lateral thickness gradients have been successfully obtained on a single substrate. Since the diffusive spread of the plasma into the reaction chamber reduces the densities of reactive species and ions along the plasma flow, the film growth rate gradually decreases with the increase of the distance from the plasma source. Therefore insight into the process of the *c*-BN film growth can be obtained by analyzing the deposited films as a function of the distance from the plasma source. Preliminary study has revealed that, under the optimal deposition condition, single-phase *c*-BN grows on the initially deposited $sp^2$-bonded BN layer with a critical $sp^2$-BN-thickness of several ten nm [6]. Recently several researchers have investigeted the initial $sp^2$-bonded BN layer by using TEM in order to obtain informations of the *c*-BN formation mechanism [7–9]. In this article, we present detailed surface characterizations of the *c*-BN film, which was confirmed to be suitable for the investigation of the growth evolution from $sp^2$-bonded BN to *c*-BN.

# 2 Experimental

## 2.1 Film deposition

Details of the ICP–CVD apparatus were published elsewhere [2]. ICP was generated inside a 38-mm-diam BN tube by 13.56-MHz 7-kW input at $1\times10^{-3}$ Torr. Flow rates of 10 % $B_2H_6$ diluted with He, $N_2$, and Ar were 20 sccm, 1.2 sccm and 2 sccm, respectively. A silicon (100) substrate was set at an angle of 45° to the axis of the plasma source so that the film was deposited on the substrate at different rates, depending on the lateral position. The distance from the top of the substrate $L$ is schematically illustrated in Fig. 1. The substrate temperature was maintained at 900 °C and the dc self-bias of -20 V was induced by applying an auxiliary rf power to the substrate. Since the plasma potential is as high as around 90 V in this experiment with regard to the grounded chamber, the sheath potential is expected to be around 110 eV. Film deposition was carried out for 10 min.

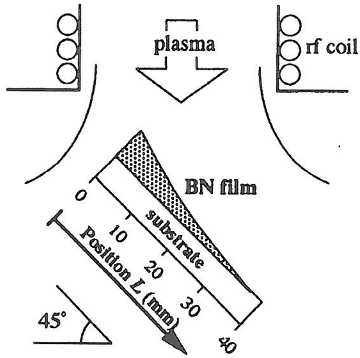

Figure 1: Schematic configuration of the ICP source and the substrate.

## 2.2 Film characterization

The polymorphism of the deposited film was analyzed by micro Fourier transform infrared (FT-IR) spectrometer (JASCO FT/IR-700). The standard analyzing area was 100×100 $\mu m^2$. The absorbances at about 1080 $cm^{-1}$ and at about 1370 $cm^{-1}$ were taken as a quantitative measure of *c*-BN and $sp^2$-bonded BN, respectively. The $sp^2$-bonded phases are known to exist as hexagonal [graphitic or turbostratic] BN (*h*-BN) or amorphous BN (*a*-BN). Reflection high energy electron diffraction patterns were obtained by using a Shimadzu $\mu$RHEED–2. Position resolved X-ray photoelectron spectroscopy (XPS) measurements were carried out with a Shimadzu/Kratos AXIS-HS facility to investigate the composition and the chemical state of the film surface. XPS spectra were obtained with nonmonochromatized Mg $K_\alpha$ radiation (1242.6 eV) with the analyzer operating at 80 eV pass energy providing 0.1 eV energy resolution. Auger electron spectroscopy measurement was carried out in JEOL JAMP-7100E. Auger transitions were excited by an electron beam of $I_P$= 1 $\mu$A at 10 kV. The surface morphology of the deposited film was observed by atomic force microscopy (AFM). The AFM used in this study was Nanoscope II (Digital Instruments, Inc.) operated in air. Images were acquired using a single crystal silicon force sensor (half-angle: 18°, the nominal radius of curvature: 5–20 nm, and the nominal force constant: 0.18 N/m) in "constant force" mode.

# 3 Results and Discusssion

## 3.1 Fourier-transform infrared spectroscopy

Figure 2 (a) shows the IR absorbance at ~1080 $cm^{-1}$ (*c*-BN) and at 1370 $cm^{-1}$ ($sp^2$-bonded BN) plotted against *L*. Basically three different growth regions can be distinguished on the sample. In the region I at large distances *L*, $sp^2$-bonded BN is formed. In the middle region II, localized formation of *c*-BN occurs on *h*-BN. In this regime both *h*-BN and *c*-BN grow on the film surface at the same time. In the region III at low distances *L*, the film surface is completely covered with cubic phase. From the result of FT-IR analysis, the structure of the sample examined in this study is expected as schematically shown in Fig. 2 (b). Labels indicates the representative positions where further surface analyses were carried out.

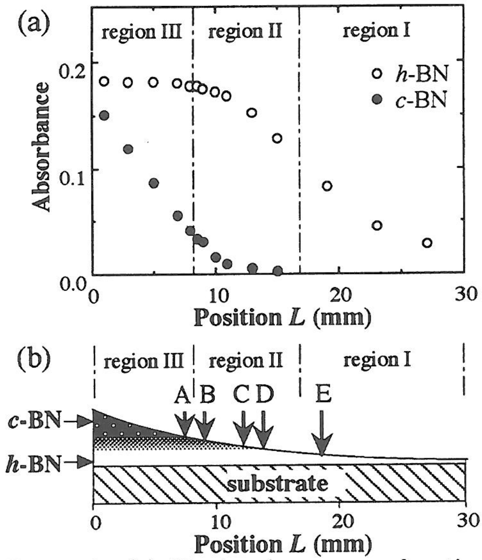


Figure 2: (a) IR absorbance as a function of the distance *L*. (b) Schematic illustration of the analyzed sample.

## 3.2 Reflection high energy electron diffraction

Figure 3 shows RHEED patterns from the BN film at different growth stages. The patterns obtained at the positions E and D show the h-BN (002) and (100) rings, while only a diffuse ring from *c*-BN (111) is observed in the pattern obtained at the position A. These patterns are consistent with the results of FT-IR analysis.

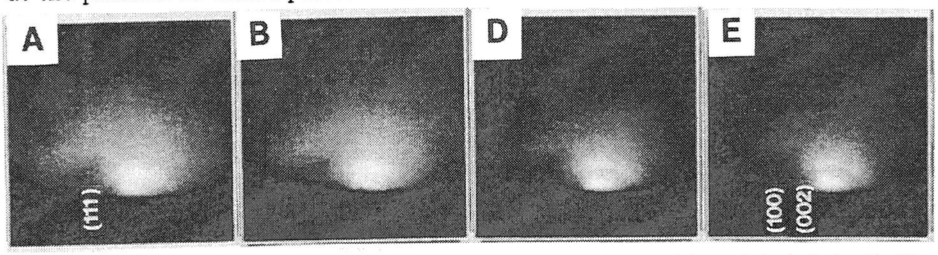


Figure 3: RHEED patterns from the BN film at the positions labeled A, B, D and E in Fig. 2 (b).

### 3.3 Auger electron spectroscopy

Figure 4 shows the Auger B *KVV* and N *KVV* spectra obtained at the positions A, B, C, D, and E. In the literature, it is reported that Auger B *KVV* line shapes of *c*-BN and *h*-BN differ significantly [10]. The Auger line shapes at the positions D and E are in good agreement with those of *h*-BN. As the *c*-BN growth proceeds, some of shoulder peaks, e.g., the high energy shoulder (180 eV) in the B *KVV* spectrum and the $\pi$ plasmon loss feature (374 eV) in the N *KVV* spectrum gradually disappear. However, it should be noted that even the Auger spectra at the position A are not identical with those for bulk *c*-BN found in the literature, but are rather similar to those for *h*-BN. Hence there might exist a rather thin surface layer of $sp^2$-bonded BN.

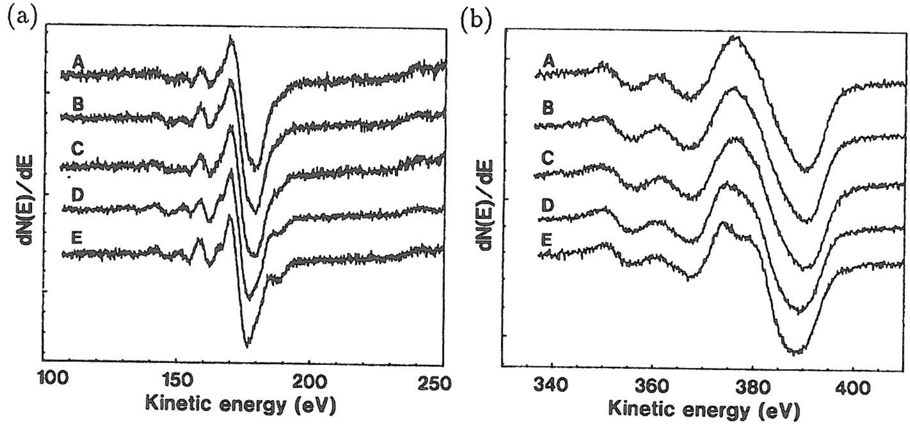


Figure 4: Auger spectra of (a) B *KVV* and (b) N *KVV*.

### 3.4 X-ray photoelectron spectroscopy

Figure 5 shows B1*s* XPS spectra obtained at the positions A, B, C, D and E. It is known that the $\pi$ plasmon loss ($\pi$P) peak occurs at 9 eV higher binding energy than the core peak for *h*-BN. Therefore $\pi$P peak can be utilized to examine the existence of *h*-BN at the surface region. The *c*-BN fraction at the surface was approximately estimated from the $\pi$P peak intensity in B1*s* and N1*s* XPS spectra. As shown in Fig. 6, the very close correlation between Ar incorporation and the estimated *c*-BN fraction has been revealed. The Ar concentration was lower than the detection limit at the initial $sp^2$-bonded BN layer, while approximately 0.4 atomic % Ar was detected at the film surface fully covered with the cubic phase. The close correlation between Ar incorporation and *c*-BN fraction at the film surface indicates that Ar is more easily entrapped during the *c*-BN growth than during the *h*-BN growth. The Ar incorporation in *c*-BN is regarded as significant since it may be a dominant cause of the significant compressive stress in the *c*-BN film.

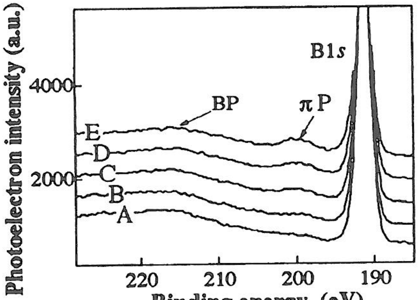


Figure 5: XPS spectra of B1*s* core level.

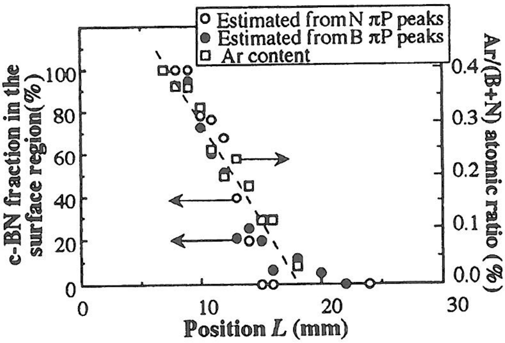


Figure 6: Ar concentration and *c*-BN fraction at the surface.

### 3.5 Atomic force microscopy

Figure 7 shows the perspective AFM images corresponding to the sequence of the initial *c*-BN growth. The surface roughness decreases drastically as the *c*-BN growth proceeds. It appears that the *c*-BN growth preferentially occurs at the concavely curved sites on the film surface.

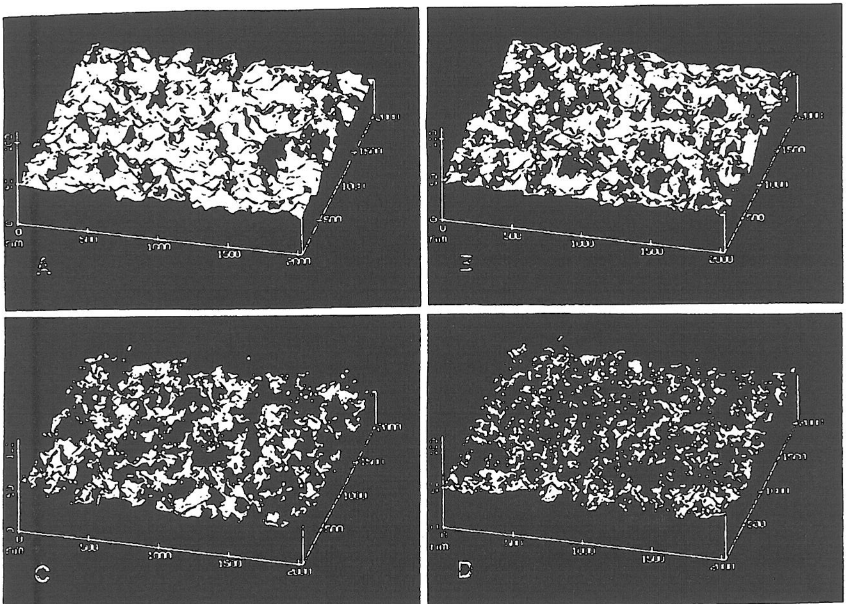


Figure 7: AFM images of the BN film at the positions labeled A, B, C and D in Fig. 2 (b). Horizontal scale: 2000 nm, vertical scale: 100 nm, perspective view.

## 4 Conclusion

The initial growth stage of *c*-BN films has mainly been studied by analyzing the film deposited on tilted silicon substrates utilizing the diffusion of a high-density plasma. The consecutive phase evolution from an initial $sp^2$-bonded BN (*a*-BN and *h*-BN) layer to single-phase *c*-BN was confirmed by FT-IR, RHEED, AES and XPS. AFM observation revealed the evolution of the surface morphology, which is characterized by drastic decrease of roughness at the transition of the growth mode from $sp^2$-bonded BN to *c*-BN. In addition, XPS measurement revealed that Ar is more easily entrapped in the film during the *c*-BN growth than during the *h*-BN growth.

## 5 Acknowledgement

The authors are grateful to thank Mr.T.Choso and Dr.M.Ohyabu, Shimadzu corporation, for XPS measurements and to Mr.T.Marui, Shimadzu corporation, for RHEED measurements.

# References

[1] T.Ichiki and T.Yoshida, Proc. 11th Int. Symp. Plasma Chem., Loughborough U.K., 1022 (1993).

[2] T.Ichiki and T.Yoshida, Appl. Phys. Lett. **64**, 851 (1994).

[3] T.Ichiki, T.Momose and T.Yoshida, J. Appl. Phys. **75**, 1330 (1994).

[4] T.Ichiki and T.Yoshida, Jpn. J. Appl. Phys. **33**, 4385 (1994).

[5] H.P.Lang, H.Haefke, G.Leemann and H.-J.Güntherodt, Physica C **194**, 81 (1992).

[6] T.Ichiki, S.Amagi and T.Yoshida, Proc. 7th Symp. Plasma Sci. Mater. p.119 (1994).

[7] D.J.Kester, K.S.Ailey, R.F.Davis and K.L.More, J. Mater. Res. **8**, 1213 (1993).

[8] D.L.Medlin, T.A.Friedmann, P.B.Mirkarimi, P.Rez, M.J.Mills and K.F.McCarty, J. Appl. Phys. **76**, 295 (1994).

[9] D.L.Medlin, T.A.Friedmann, P.B.Mirkarimi, M.J.Mills and K.F.McCarty, Phys. Rev. B **50**, 7884 (1994).

[10] R.Trehan, Y.Lifshitz and J.W.Rabalais, J. Vac. Sci. Technol. A **8**, 4026 (1990).